Dependence of effective internal field of congruent lithium niobate on its domain configuration and stability

Ranjit Das, Souvik Ghosh, and Rajib Chakraborty

Citation: Journal of Applied Physics **115**, 243101 (2014); doi: 10.1063/1.4885042
View online: http://dx.doi.org/10.1063/1.4885042
View Table of Contents: http://scitation.aip.org/content/aip/journal/jap/115/24?ver=pdfcov
Published by the AIP Publishing

Dependence of effective internal field of congruent lithium niobate on its domain configuration and stability

Ranjit Das,[a] Souvik Ghosh,[a] and Rajib Chakraborty[a]
Department of Applied Optics & Photonics, University of Calcutta, JD-2, Sector III, Salt Lake, Kolkata 700098, India

(Received 15 May 2014; accepted 13 June 2014; published online 23 June 2014)

Congruent lithium niobate is characterized by its internal field, which arises due to defect clusters within the crystal. Here, it is shown experimentally that this internal field is a function of the molecular configuration in a particular domain and also on the stability of that particular configuration. The measurements of internal field are done using interferometric technique, while the variation of domain configuration is brought about by room temperature high voltage electric field poling. © *2014 AIP Publishing LLC*. [http://dx.doi.org/10.1063/1.4885042]

I. INTRODUCTION

For the last few decades, Lithium Niobate ($LiNbO_3$) is one of the most important ferroelectrics in optoelectronics and nonlinear optics. Its properties are of vast significance to fundamental and applied optics research and are employed in several acousto-optic, electro-optic, and nonlinear optical devices such as modulators of light, beam deflector, optical frequency converters, tunable sources of coherent light, etc.[1–4] While devices fabricated on stoichiometric or near-stoichiometric crystals are less prone to photorefractive damage[5,6] but production of such crystals requires expensive procedures and precise control over mass production, bringing up the crystal price.[7–10] So, most of the devices are made on congruent $LiNbO_3$.

$LiNbO_3$ crystal is characterized by its Curie temperature, which indeed reflects the congruency of the molecular organization in the crystal.[11] Also asymmetry in hysteresis loop measured during forward and backward poling gives an estimation of the internal structure of the crystal. It is well known that this asymmetry in hysteresis loop is due to the existence of internal field in the ferroelectric crystal. So, a proper analysis of the asymmetry of the hysteresis loop would result in the measurement of internal field of the crystal.[12,13] The presence of internal field in $LiNbO_3$ is due to co-existence of spontaneous polarization due to inherent shifted positions of Nb^{5+} and Li^{+} ions and defect state polarization, which is due to presence of defect clusters Li^{+} ion vacancies and Nb-antisites.[14]

The strength of internal field has been studied by successive forward and reverse poling of the crystal.[12,13] For inspection of the internal field in a patterned domain $LiNbO_3$, this technique may destroy the structure. Also, the thin wafers are susceptible to damage due to high electric field. Consequently, interferometric techniques, which are non-destructive techniques, have been developed for quantitative measurement of internal field in ferroelectric crystals.[15–18] The authors have also proposed[19] an interferometric technique to measure internal field, which have several advantages over the methods used in Refs. 15–18.

In this work, quantitative assessment of the dependence of internal field on domain configuration and stability has been studied. For that, the internal fields in single domain $LiNbO_3$, domain inverted $LiNbO_3$ and unstable domain inverted or the so called frustrated domain inverted $LiNbO_3$ crystals are measured using interferometric technique and compared. It is seen that the magnitude of internal field (IF) of single domain and domain inverted $LiNbO_3$ are the same. Only their directions are reversed as the axes are opposite for the two cases. But in frustrated domain inverted $LiNbO_3$, the effective internal field is considerable different. Moreover, its value also varies with time as this frustrated state is unstable, bouncing back to its initial as-bought single domain state after some time. Possible reasons for the observations are explained using the defect model.

II. MEASUREMENT SETUP AND TECHNIQUE USED

The measurement of internal field is done using the Mach-Zehnder Interferometric (MZI) setup, which is schematically shown in Fig. 1. The probe beam is obtained from a He-Ne laser source having wavelength of 632.8 nm. A beam splitter is used to split the probe beam along two mutually perpendicular paths. Two mirrors are used to

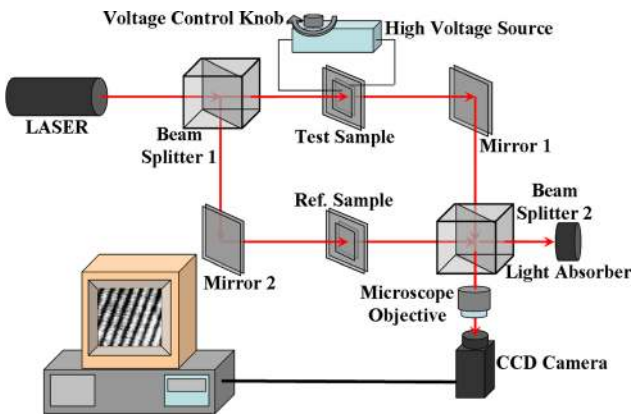

FIG. 1. Setup for the measurement of internal field in $LiNbO_3$ crystals.

[a]Electronic addresses: ranjitdas.in@gmail.com, souvik2cat@gmail.com, and srirajib@yahoo.com

deflect these beams and combine on a second beam splitter. A fringe pattern is, thus, produced. A microscope objective is placed along the path of output beam from the last beam splitter to magnify the output fringe pattern and, then, the resulting fringe pattern is recorded with the help of a CCD camera. The test sample, which is coated with a semi-transparent aluminum (Al) coating on both faces with provision to apply high voltages across it, is placed in one arm. A similar type of sample, but without the provision for applying high voltage, is used as reference and is kept in the reference arm of the interferometer. The aim of using reference sample is to minimize any natural or atmospheric influence that may alter crystal parameters affecting output fringe pattern. Moreover, it is used to match the intensities of test beam and reference beam. Positioning of the samples in the respective arms is critical and care should be taken such that the crystallographic c-axes of the samples coincide with the direction of probe beams to minimize the complexity of the analysis. Otherwise, the probe beam will have two sets of polarization and its effect should be considered. Photorefractive damage of the crystal does not arise as the laser beam intensity is quite low and is further lowered due to splitting of source beam by first beam splitter and subsequent reduction by the semitransparent Al-coatings as electrodes on the sample surfaces. Moreover, as mentioned in Ref. 20, the absorption of He-Ne laser source at 632.8 nm is low, thus, reducing both photorefractive and photovoltaic effect. Also, Al-coating being thermally conducting, laser heating of sample surfaces is reduced; so Al-coatings can act as heat sinks here and pyroelectric effect can be avoided. The output of the interferometer is a fringe pattern, which is a function of applied voltage across the test sample. In this regard, it should be noted that no voltage should be applied across the reference sample. So any variation in the output fringe pattern is only due to the electro-optic response of the test sample.

Determination of internal field is based on the measurement of the fringe shift due to the applied field on the test sample. Due to electro-optic property of the crystal, the applied field causes a change in refractive index of the crystal (Δn), which causes a phase shift ($\Delta\Phi$) between the two interfering beams resulting in the fringe pattern. The applied field for the fringe shift due to halfwave (or 180°) phase change is called halfwave field (E_π) and can be represented as[21]

$$E_\pi = \frac{\lambda}{r_{13} n_o^3 d}, \tag{1}$$

where λ is the free space wavelength of the probe beam, d is the crystal width, r_{13} and n_o are the respective electro-optic coefficients and ordinary refractive index of $LiNbO_3$ at that wavelength. Now, if $E_{\Delta\Phi}$ and $E'_{\Delta\Phi}$ are the applied field in the forward and reverse directions, respectively, for a phase change $\Delta\Phi$ of the fringe pattern, the internal field (E_{int}) will be[19]

$$E_{int} = \alpha \frac{\left(E_{\Delta\Phi} - E'_{\Delta\Phi}\right)}{(\Delta\Phi/\pi)}, \tag{2}$$

where α is a constant having value equal to the thickness (in mm unit). Although $LiNbO_3$ is also a piezo-electric material, as explained in Ref. 19, this property will not affect the internal field here.

III. EXPERIMENTAL RESULTS AND DISCUSSIONS

The experiments were performed on square shaped samples (10.0×10.0) mm^2, which are obtained by slicing them from circular (3 in. diameter), z-cut single domain $LiNbO_3$ crystal wafers of thickness of either 0.5 mm or 1.0 mm. The electric field is applied along the crystallographic c-axis, where the velocity of ordinary ray and that of extraordinary ray matches, so $n_o = n_e = 2.28$, while the corresponding electro-optic coefficient will be r_{13}, whose value is considered as 10×10^{-12} m/V.[17] Semi-transparent aluminum electrodes of rectangular shape are defined on the central portion of both the surfaces of the samples by proper masking so that they cover 50% of the sample surface. The experiment consists of measurement of electric field corresponding to half-wave phase change in both forward and reverse directions of different samples.

Initially, the test is done using as-bought single domain $LiNbO_3$ samples of thickness 0.5 mm. Before making any experiment using as-bought samples, they are annealed at a temperature of 200 °C for about 30 min and, subsequently, cooled down to room temperature. To apply electric field along the z-axis (which is also the optic axis) of the crystal, the electrode designed at +z surface of the test sample is connected with the positive terminal of the high voltage source and the electrode designed at the –z surface of the same is connected with the negative terminal of the source. Halfwave field (E_π) is measured to be 11.0 ± 0.1 KV/mm, in this case. The fringe pattern for zero applied field is shown in Fig. 2(a), while for halfwave field (E_π), it is shown in Fig. 2(b). On comparing the two fringe patterns, a 180° phase shift corresponding to halfwave field can be clearly observed. After this measurement, the test sample is kept idle for about 1 h with its electrodes shorted and grounded, such that the sample is allowed to relax back to its initial

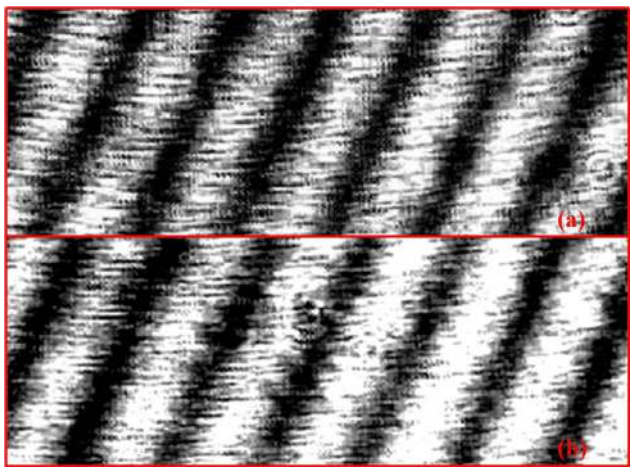

FIG. 2. A typical observed fringe pattern obtained from the MZI setup for (a) zero applied filed and (b) applied field for half wave phase shift. Similar fringe pattern can be obtained for different types of $LiNbO_3$ crystals.

condition and any accumulation of charge in the sample may drain out. Again, the test sample is annealed at a temperature of 200 °C for about 30 min and, consequently, brought down to room temperature. Next, the polarities of the electrical connections to the test samples are interchanged so that half-wave field (E'_π) along reverse z-direction can be determined and the value is measured to be 6.0 ± 0.1 KV/mm. Similar shift of fringe pattern as that in Fig. 2 is observed here also. The above steps are followed again for samples of thickness 1.0 mm and nearly repeatable results are obtained.

In an attempt to test the effect of domain inversion and domain stability on internal field, the test samples, which are initially single domain, are domain inversed using room temperature high voltage electric field poling. Room temperature domain inversion generally produces complete and permanent domain inverted crystal, if the poling is done over whole surface of the sample.[22] But stability of domain inverted structure depends on the presence of anti-parallel domains in its vicinity if poling is done over some limited region of the sample, which is the case for the sample used here. In that case, permanent inverted domains can only be obtained by thermal annealing of the poled crystal at about 200 °C for 30 min. Otherwise, the inverted domain would be unstable and return back to the initial as-bought single domain condition. As already mentioned, this is the so called frustrated domain inverted state of $LiNbO_3$.

Stable or permanent domain inverted sample so obtained is, then, placed in the test arm of the MZI setup and its corresponding halfwave field values ($E_{P\pi}$, $E'_{P\pi}$) are noted by observing and comparing output fringe patterns due to applied electric fields across it. Results of particular interest are the halfwave field values ($E_{F\pi}$, $E'_{F\pi}$) obtained for unstable (frustrated) domain inverted samples. The phase shift due to gradual increment of applied electric field in forward as well as reverse direction for single domain, permanent domain inverted, and unstable domain inverted $LiNbO_3$ crystals is shown in Fig. 3. As the increment of phase with applied electric field along forward direction is considered positive, the increment of phase in the reverse direction is to be considered as negative. So, both positive and negative values of phases with change of magnitude of electric field are plotted in this figure.

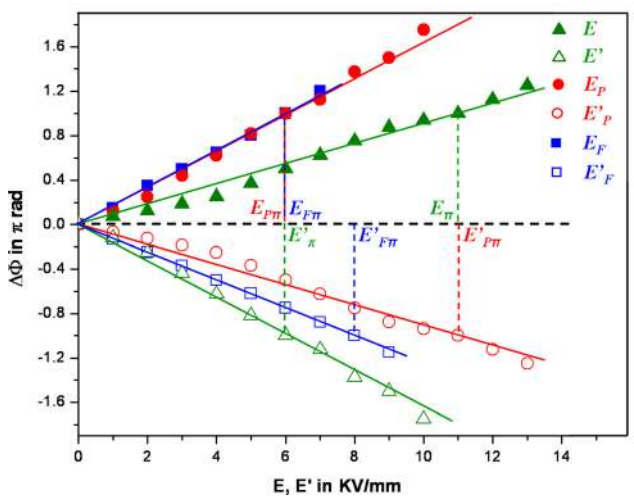

FIG. 3. Phase variation with the applied field for as-bought $LiNbO_3$ crystal (green line), stable domain inverted $LiNbO_3$ crystal (red line), and frustrated domain inverted $LiNbO_3$ crystal (blue line).

The set-up for high voltage electric field poling, which is utilized for the production of permanent and frustrated domain inverted $LiNbO_3$, is shown in Fig. 4. As high fields of the order of 22 KV/mm (greater than the coercive field, i.e., 21 KV/mm in case of $LiNbO_3$) is to be applied across the samples, they are kept insulated inside a rubber jacket so that unwanted air breakdown around the samples may be avoided to protect them from cracking down. The current meter is used here mainly to indicate the completeness of domain inversion of the test sample. After setting up the circuit shown in Fig. 4, the high voltage source is switched ON and the output voltage level is gradually increased. There will be practically no current detected by the current meter until the voltage level is greater than 10.5 KV (approximately) for samples of thickness 0.5 mm. But, at or beyond that value of applied voltage, there will be a displacement current, which can be detected by the current meter. After completion of domain inversion, the displacement current turns out to be zero again.

As given in Sec. II, the values of internal field for as-bought, stable domain inverted, and frustrated domain inverted $LiNbO_3$ crystals are calculated using Eq. (2), from the corresponding halfwave field values. Internal fields obtained in the three cases for 0.5 mm thick $LiNbO_3$ crystal are tabulated in Table I. It is noteworthy that in the case of frustrated domain inverted sample, the timings of measurement of halfwave fields play an important role. If immediately after domain inversion, the sample is placed in the MZI setup and the halfwave fields are measured, the magnitude of IF so achieved is much lower than that obtained for stable domain inverted sample. On the other hand, if frustrated domain inverted sample is tested in the same MZI setup after a long time interval (say about 24 h), after domain inversion it is observed that its IF comes out to be as that obtained for as-bought single domain samples.

From Table I, it is seen that the magnitude of the effective internal field in complete domain inverted crystal is approximately same as that of the as-bought single domain crystal. But, as complete domain inversion reorients the molecular configuration in the opposite direction, the sign of the internal field gets reversed. On the other hand for frustrated domain inverted sample, the magnitude of effective internal

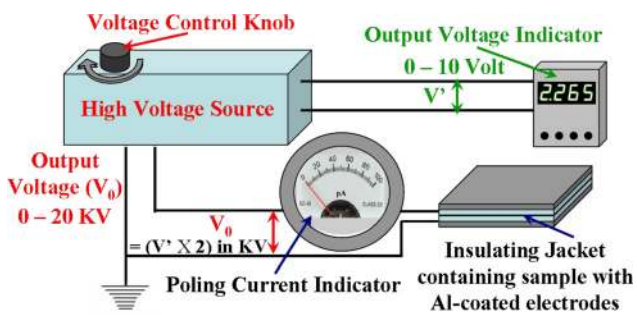

FIG. 4. High voltage electric field poling setup.

TABLE I. Measured values of internal field for $LiNbO_3$ sample of thickness 0.5 mm.

			Frustrated domain inverted $LiNbO_3$ crystal	
	As bought $LiNbO_3$ crystal	Complete domain inverted $LiNbO_3$ crystal	Immediately after poling	24 h after poling
E_π in kV/mm	10.8	6.0	6.0	11.0
E_π' in kV/mm	6.0	11.0	8.0	6.2
E_{IF} in kV/mm	2.4	−2.5	−1.0	2.4

field is reduced significantly. These observed phenomena can be understood with the help of a defect cluster model suggested by Gopalan *et al.*[14] According to this model, the presence of defects in congruent $LiNbO_3$ plays an important role for observation of internal fields in such crystals. At equilibrium, a combined effect of polarization field due to inherent molecular arrangement and depolarizing field due to defect clusters produces a resultant electric field inside the crystal, which is known as the internal field. Domain inversion by high electric field poling of the crystal creates a reorientation of the defect clusters inside the bulk crystal. If the poling conditions are controlled in such a way that all the defect clusters find stable positions inside the crystal so that no further movement of those clusters occur, the resultant crystal will be in permanent domain inverted state. A simple scheme to obtain permanent domain inversion is to anneal the poled crystal, which forces the defect clusters to move to those minimum energy positions, which should be occupied by them after complete domain inversion. On the other hand, if annealing treatment is not followed after poling of the sample, there are notable movements of those defect clusters inside the crystal and the resulting domain may return back to its initial as-bought single domain state. It should be noted that room temperature high electric field domain inversion over whole crystal generally produces permanent domain inversion without applying annealing treatment on poled samples. But here, in this work, the poling is intentionally done over some limited region (about 50%) of the sample so that unstable or frustrated domain inversion of the crystal can be done. It is shown, in this work, that subsequent annealing of the poled sample at 200 °C for about 30 min can produce permanent domain inverted crystal. Also for the poled sample, where annealing is not followed, it is observed that the same has returned back to the as-bought sample condition. Time evolution of the effective IF of un-annealed or the so called frustrated domain inverted sample certainly proved that the crystal move to the as-bought single domain state from the frustrated state after some relaxation time. This observation taken 24 h after poling is also reported in Table I.

IV. CONCLUSIONS

Study of the dependence of IF in $LiNbO_3$ under various conditions of the domain orientation and stability inside the crystal is done. Time evolution of IF in frustrated domain inverted $LiNbO_3$ is also performed and reported. A detailed and precise work on time evolution of IF is to be carried out in future for complete understanding of unstable domain inverted $LiNbO_3$ crystals and internal mechanism of electric field domain inversion of ferroelectrics and subsequent domain stability. But still with the stated technique variation of effective IF under various domain orientation and stability is successfully measured and reported. A defect model suggested by Gopalan *et al.*[14] is utilized here to explain the outcome of the time evolution.

ACKNOWLEDGMENTS

This work was supported by Department of Science & Technology, Government of India (Grant No. SR/S2/LOP-15/2009).

[1]H. Nishihara, M. Haruna, and T. Suhara, *Optical Integrated Circuit* (McGraw-Hill, 1989).
[2]A. Yariv and P. Yeh, *Optical Waves in Crystals* (John Wiley and Sons, 1984), Chap. 4, 7, and 8.
[3]K. Suizu and K. Kawase, "Monochromatic-tunable terahertz-wave sources based on nonlinear frequency conversion using lithium niobate crystal," IEEE J. Sel. Top. Quantum Electron. **14**, 295–306 (2008).
[4]Y. Y. Lin, S. T. G. W. Chang, A. C. Chiang, Y. C. Huang, and Y. H. Chen, "Electro-optic periodically domain inverted lithium niobate Bragg modulator as a laser Q-switch," Opt. Lett. **32**, 545–547 (2007).
[5]A. Ashkin, G. D. Boyd, J. M. Dziedzic, R. Smith, A. A. Ballman, J. J. Levinstein, and K. Nassau, "Optically induced refractive index inhomogeneities in $LiNbO_3$ and $LiTaO_3$," Appl. Phys. Lett. **9**, 72–73 (1966).
[6]D. A. Bryan, R. Gerson, and H. E. Tomaschke, "Increased optical damage resistance in lithium niobate," Appl. Phys. Lett. **44**, 847–849 (1984).
[7]K. Kitamura, J. K. Yamamoto, N. Iyi, S. Kimura, and T. Hayashi, "Stoichiometric $LiNbO_3$ single crystal growth by double crucible Czochralski method using automatic power supply system," J. Cryst. Growth **116**, 327–332 (1992).
[8]P. F. Bordui, R. G. Norwood, D. H. Jundt, and M. M. Fejer, "Preparation and characterization of off-congruent lithium niobate crystals," J. Appl. Phys. **71**, 875–879 (1992).
[9]I. Pracka, A. L. Bajor, S. M. Kaczmarek, M. Wirkowicz, B. Kaczmarek, J. Kisielewski, and T. Ukasiewicz, "Growth and characterization of $LiNbO_3$ single crystals doped with Cu and Fe ions," Cryst. Res. Technol. **34**, 627–634 (1999).
[10]R. Mouras, M. Fontana, P. Bourson, and A. Postnikov, "Lattice site of Mg ion in $LiNbO_3$ crystal determined by Raman spectroscopy," J. Phys.: Condens. Matter **12**, 5053–5060 (2000).
[11]M. N. Palatnikov, N. V. Sidorov, V. I. Skiba, D. V. Makarov, I. V. Biryukova, Y. A. Serebryakov, O. E. Kravchenko, Y. I. Balabanov, and V. T. Kalinnikov, "Effects of nonstoichiometry and doping on the Curie temperature and defect structure of lithium niobate," Inorg. Mater. **36**, 489–493 (2000).
[12]L.-H. Peng, Y.-C. Fang, and Y.-C. Yin, "Polarization switching of lithium niobate with giant internal field," Appl. Phys. Lett. **74**, 2070–2072 (1999).
[13]V. Gopalan, T. E. Michell, Y. Furukawa, and K. Kitamura, "The role of nonstoichiometry in 180° domain switching of $LiNbO_3$ crystals," Appl. Phys. Lett. **72**, 1981–1983 (1998).
[14]V. Gopalan, V. Dierolf, and D. A. Scrymgeour, "Defect-domain wall interactions in trigonal ferroelectrics," Annu. Rev. Mater. Res. **37**, 449–489 (2007).
[15]Q. Chen and D. Stencil, "Identification and quantitative characterization of antiparallel domains using an interferometric method," Appl. Opt. **33**, 7496–7499 (1994).
[16]M. Paturzo, D. Alfieri, S. Grilli, P. Ferraro, P. De Natale, M. de Angelis, S. De Nicola, A. Fiñizio, and G. Pierattini, "Investigation of electric internal field in congruent $LiNbO_3$ by electro-optic effect," Appl. Phys. Lett. **85**, 5652–5654 (2004).

[17]M. de Angelis, S. De Nicola, A. Finizio, G. Pierattini, P. Ferraro, S. Grilli, and M. Paturzo, "Evaluation of the internal field in lithium niobate ferroelectric domains by an interferometric method," Appl. Phys. Lett. **85**, 2785–2787 (2004).
[18]Y. Zhi, D. Liu, W. Qu, Z. Luan, and L. Liu, "Investigation of effective internal field in congruent lithium niobate crystal by digital holographic interferometry," Appl. Phys. Lett. **90**, 032903 (2007).
[19]R. Das and R. Chakraborty, "Interferometric measurement of internal field of lithium niobate without high voltage electric field poling," Opt. Eng. **53**, 054105–1–054105–6 (2014).
[20]S. T. Popescu, A. Petris, and V. I. Vlad, "Interferometric measurement of the pyroelectric coefficient in lithium niobate," J. Appl. Phys. **113**, 043101–1–043101–4 (2013).
[21]R. Das and R. Chakraborty, "Enhanced electro-optic property in $LiNbO_3$ by electric field domain inversion," IEEE Photon. Technol. Lett. **25**, 1626–1628 (2013).
[22]F. Yazdani, M. L. Sundheimer, and A. S. L. Gomes, "Ferroelectric domain inversion in congruent lithium niobate," in *Proceedings of the SBMO/IEEE MTT-S International Conference on Microwave and Optoelectronics, 20–23 September 2003* (2003), Vol. 1, pp. 453–458.